Title

EDTA functionalized magnetic nanoparticle sorbents for cadmium and lead contaminated water treatment

Authors

Huang, Yuxiong
Keller, Arturo A

Publication Date

2015-09-01

DOI

10.1016/j.watres.2015.05.011

Peer reviewed

Available online at www.sciencedirect.com

ScienceDirect

journal homepage: www.elsevier.com/locate/watres

EDTA functionalized magnetic nanoparticle sorbents for cadmium and lead contaminated water treatment

*Yuxiong Huang, Arturo A. Keller**

Bren School of Environmental Science and Management, University of California at Santa Barbara, CA 93106, USA

ARTICLE INFO

Article history:
Received 8 April 2015
Received in revised form
4 May 2015
Accepted 5 May 2015
Available online 10 May 2015

Keywords:
Nanoparticle
EDTA
Metal decontamination
Magnetic separation
Sorption
Regeneration

ABSTRACT

Cadmium (Cd^{2+}) and lead (Pb^{2+}) are toxic to human beings and other organisms, and the U.S. Environmental Protection Agency (EPA) has classified both as probable human carcinogens. In this study, a regenerable magnetic ligand particle (Mag-Ligand) which includes a metal-binding organic ligand (EDTA) attached to an iron oxide nanoparticle was developed for rapid removal of Cd^{2+} and Pb^{2+} as well as other metals from contaminated water. Mag-Ligand showed fast removal ability for both Cd^{2+} (<2 h) and Pb^{2+} (<15 min) with relatively high sorption capacity (79.4 and 100.2 mg/g for Cd^{2+} and Pb^{2+}, respectively). The removal performance of Mag-Ligand was high across a wide pH range (3–10) as well as in the presence of competitive metal ions (Ca^{2+} and Mg^{2+}). In addition, Mag-Ligands can be easily regenerated (washed by 1% HCl) and reused several cycles with high sorption capacity. This study indicated that Mag-Ligand is a reusable sorbent for rapid, convenient, and efficient removal of Cd^{2+} and Pb^{2+} from contaminated aquatic systems.

1. Introduction

Heavy metal ions such as cadmium (Cd) and lead (Pb) are considered as serious threat to the environment and human health due to their high toxicity and non-degradable characteristics (Kah et al., 2012). Cd can be released into the environment both from natural sources (e.g. volcanic eruptions and forest fires) (Bandara et al., 2008) and anthropogenic activities (e.g. non-ferrous metals production (Vromman et al., 2008), electroplating (Islamoglu et al., 2006), manufacturing of Ni–Cd batteries and pigments (Fthenakis, 2004), application of phosphate fertilizers (Mortvedt and Osborn, 1982), and burning of fossil fuels (Vouk and Piver, 1983)). Pb also is emitted from natural sources and anthropogenic activities (e.g. lead-based batteries, residual lead paint, lead-based fuel additives) (Reimann and de Caritat, 2005). They are bioaccumulated (Tête et al., 2014), so even at trace levels they can concentrate in living organisms acting as carcinogens. For example cadmium may cause damage to lungs (Boudreau et al., 1988), kidneys (Jamall et al., 1989), livers (Koyuturk et al., 2007), and reproductive organs (Alvarez et al., 2004; Bonda et al., 2004). Recently, studies have been reported that grains such as rice and soybean have been contaminated by cadmium (Su et al., 2014), and this has become an emerging food chain supply threat, especially in Asian countries (Shute and Macfie, 2006). On the other hand, lead contamination could occur when water flows through lead-containing pipes

* *Corresponding author*. Tel.: +1 805 893 7548; fax: +1 805 893 7612.
E-mail address: keller@bren.ucsb.edu (A.A. Keller).
http://dx.doi.org/10.1016/j.watres.2015.05.011
0043-1354/

(Xie and Giammar 2011), which also would enter the food chain through drinking water. Therefore, to develop effective and rapid cadmium and lead remediation technique is of great importance.

Chelating agents, for instance ethylenediaminetetraacetic acid (EDTA), are widely used as extractive reagents for heavy metals decontamination (Martinez et al., 2006; Ngah and Hanafiah, 2008). Due to its strong metal chelating ability and low cost, EDTA has been used to functionalize a variety of materials from inorganic oxides to biomass, including silica gel (Repo et al., 2009), chitosan (Repo et al., 2010), polyamine composites (Hughes and Rosenherg, 2007), polystyrene (Wang et al., 2010), mercerized cellulose and sugarcane bagasse (Júnior et al., 2009), wood sawdust and sugarcane bagasse (Pereira et al., 2010), rice husk (Xiong et al., 2010), and baker's yeast biomass (Yu et al., 2008). However, a comparison of results shows that the adsorption efficiency was significantly influenced by the type of supporting material (Repo et al., 2011), and post-treatment separation needs to be taken into consideration.

In the past few years, nano-scaled magnetic particles have been proposed as sorbents for environmental decontamination (Huang and Keller, 2013; Su et al., 2015), and due to their superparamagnetic nature as well as their unique physical and chemical properties such as high dispersibility, relatively large surface area, and high ratio of surface-to-volume, they exhibit a high adsorption capacity (Bagheri et al., 2012). With an appropriate coating, which can be either inorganic (e.g., silica or alumina) (Jiang et al., 2012; Karatapanis et al., 2011) or organic (e.g., modified with polymer or surfactant, etc.) (Faraji et al., 2010; Huang et al., 2010), these magnetic core hybrid particles can be applied to remove heavy metal ions (Ge et al., 2012), hydrophobic compounds (Wang et al., 2008), pesticides (Clark and Keller, 2012b), natural organic matter (Wang et al., 2011), oxyanions (Clark and Keller, 2012a) and emerging organic contaminants (Huang and Keller, 2013).

Recent studies investigated EDTA-modified magnetic nanoparticles for metals remediation. Zhang et al. (2011) reported a route for EDTA immobilization on the surface of amine-terminated Fe_3O_4 nanoparticles (Fe_3O_4–NH_2/PEI-EDTA) for treatment of Cu^{2+}, Cd^{2+}, and Pb^{2+} from aqueous solutions. The results suggested that solution pH plays an important role on removal efficiency, with 98.8% Pb^{2+} removal at pH 5, but decreasing removal at higher pH. Dupont et al. (2014) decorated magnetic (Fe_3O_4) nanoparticles with N-[(3-trimethoxysilyl)propyl]ethylenediamine triacetic acid (TMS-EDTA) for rare earth elements adsorption, and found increasing removal of Gd^{3+} as solution pH increased. However, none of the previous researchers considered the potential competitive adsorption between heavy metal ions and Ca^{2+} or Mg^{2+}, which usually are present at much higher concentration than these trace heavy metal ions.

To decrease the impact of solution pH and water hardness (i.e. Ca^{2+} or Mg^{2+}), we developed a nanomaterial (Mag-Ligand) with a magnetic core covered by an organic ligand (EDTA) that can serve as an effective sorbent for metal ions from realistic aquatic systems. The initial application under consideration is the treatment of industrial wastewater, but Mag-Ligand could be to remove metal ions from contaminated groundwater or mining leachate. We evaluated the adsorption capacity of Cd^{2+} and Pb^{2+} onto Mag-Ligand at different initial Cd^{2+} and Pb^{2+} concentrations as well as determined the adsorption isotherms and kinetics. In addition, the remediation performance of Mag-Ligand for Cd^{2+} removal under various environmental conditions (e.g. range of pH and water hardness) as well as the regenerability and reusability were studied. The results demonstrated that Mag-Ligand is a rapid, effective, regenerable and more sustainable sorbent for Cd^{2+} and Pb^{2+} and thus a promising material for metal ion decontamination.

2. Experimental

2.1. Chemicals

Maghemite (iron (III) oxide) nanoparticles (30 nm in diameter) and pyridine were purchased from Alfa Aesar (USA). Cadmium and lead standard for AAS (1000 mg/L Cd^{2+}/Pb^{2+} in nitric acid) and (3-aminopropyl)triethoxysilane (99%) were purchased from Sigma–Aldrich (USA). Cadmium chloride anhydrous, lead chloride, ethylenediaminetetraacetic acid (EDTA), nitric acid, hydrochloric acid, citric acid, tris (hydroxymethyl)aminomethane, acetic acid, sodium bicarbonate and sodium carbonate were purchased from Fisher Scientific (USA). Diethylether and sodium dihydrogen phosphate were purchased from Acros Organics (Geel, Belgium). Sodium hydroxide and toluene were purchased from EMD Millipore (USA). All chemicals were used as received, without further purification. All solutions were prepared with deionized water (18 MΩ-cm) from a Barnstead NANOpure Diamond Water Purification System (USA).

2.2. Synthesis of Mag-Ligand

Maghemite nanoparticles (1.0 g) were dispersed into 40 mL of toluene in a flask. After mixing well, 0.4 mL of 3-aminopropyltriethoxysilane (APTES) were added to attach an amino group to the maghemite particles. Then the flask was connected to a reflux system (WU-28615-06, Cole–Parmer, USA), which was then rotated at 30 rpm (revolutions/minute) in a water bath at 90 °C, and refluxed for 2 h. After the solution cooled to room temperature (22 °C), 2 mM EDTA and 60 mL pyridine were added. The mixture was again rotated at 30 rpm in a water bath at 90 °C in the reflux system for 2 h. After the solution cooled down to room temperature, 100 mL of sodium bicarbonate (0.5 M) was added to adjust pH. A magnet (Eclipse Magnetics N821 permanent, 50 mm × 50 mm × 12.5 mm; 243.8 g; pull force: 40.1 N) was applied to the bottom of the flask to recover the nanoparticles while the supernatant was decanted. Deionized (DI) water was used to rinse the particles twice and then decanted while retaining the particles with the magnet. The same rinsing procedure was performed twice with ethanol and then diethylether. The particles were dried at room temperature for 24 h, and stored in a capped bottle prior to use.

2.3. Characterization of Mag-Ligand

Transmission electron microscopy (TEM) images were obtained using a JEOL 1230 Transmission Electron Microscope

operated at 80 kV. Scanning electron microscopy (SEM) studies were performed on an FEI XL40 Sirion FEG Digital Scanning Microscope with an Oxford EDS analysis system. The thermogravimetric analyses (TGA) were used to investigate the amount of EDTA coated on the magnetic core, using a Mettler Toledo TGA/sDTA851e apparatus with an air flow of 100 mL/min and a heating rate of 5 °C/min. Magnetization measurements were performed on a Quantum Design MPMS 5XL SQUID Magnetometer. The functional groups of the Mag-Ligand composite were detected using a Fourier transform infrared (FTIR) spectrometer on a Nicolet iS 10 FT-IR Spectrometer.

2.4. Batch sorption of Cd^{2+} and Pb^{2+}

For most experiments 5.0 mg of Mag-Ligand particles were mixed with 25 mL of Cd^{2+} or Pb^{2+} solution (10 mg/L) in 50 mL conical tubes, and the pH was adjusted to the desired condition (range from 4 to 10) by using a pH buffer. An acetic acid buffer was used for the pH interval between 3.5 and 5.5, citric acid was used for pH 6.0; pH 7.0 was obtained by using sodium dihydrogen phosphate buffer, pH between 7.5 and 9.5 was obtained by using tris (hydroxymethyl)aminomethane buffer, and sodium carbonate buffer was used to obtain pH 10.0. All buffer solutions were prepared at 100 mM concentration but the concentration of pH buffer was always kept below 10 mM to minimize other interactions. Then, these tubes were placed in an end-over-end shaker on a Dayton-6Z412A Parallel Shaft (USA) roller mixer with a speed of 70 rpm at room temperature for 24 h to ensure sufficient equilibration time. Adsorption kinetics studies were carried out at the same conditions as previously stated but for a set amount of time, varying from 15 min to 24 h, with pH = 7. After this mixing, the Mag-Ligand particles were separated from the mixture with the Eclipse magnet. All experiments were conducted at ambient temperature (22–25 °C).

The concentration of adsorbent was varied from 0.04 to 0.28 g/L to study the adsorption isotherms of Cd^{2+} or Pb^{2+} onto Mag-Ligand at pH 7. Additionally, solutions with varying initial concentrations of Cd^{2+} or Pb^{2+}, which ranged from 1 mg/L to 100 mg/L were treated with the same procedure as above at pH 7 and 5.0 mg Mag-Ligand.

In order to study the effect of ionic strength (e.g. water hardness), on the removal efficiency of Mag-Ligand, Ca^{2+} (ranging from 1 mg/L to 100 mg/L) and Mg^{2+} (ranging from 0.6 mg/L to 60 mg/L) were added to some of the experiments, at pH 7.

2.5. Regeneration and reuse of Mag-Ligand

To investigate the regeneration and reuse of Mag-Ligand, 10 mg/L Cd^{2+} were used with the same adsorption process, followed by separation of the Mag-Ligand from solution with the handheld magnet. The Mag-Ligand collected was then washed with 1% HCl (10 min, room temperature), and the Cd^{2+} concentration in the supernatant solution (the solution pH is around 1.70) was determined by ICP. The regenerated Mag-Ligand particles were then reused for subsequent Cd^{2+} sorption experiments. The sorption, extraction, and reuse processes were repeated for five times. Changes in sorption capacity and Mag-Ligand particle recovery were determined at every cycle.

2.6. Analysis

A Thermo iCAP 6300 inductively coupled plasma with atomic emission spectroscopy (ICP-AES) was used to analyze the concentration of Cd^{2+} and Pb^{2+} (Adeleye et al., 2013; Adeleye and Keller, 2014; Huang et al., 2014). All tests were performed in triplicate and analysis of variance (ANOVA) was used to test the significance of results. A $p < 0.05$ was considered to be statistically significant.

Metal ions removal efficiency and sorption capacity was calculated as:

$$Removal\ \ efficiency = \frac{C_0 - C_t}{C_0} \times 100\% \quad (1)$$

$$Sorption\ \ capacity = q_e = \frac{(C_0 - C_t)\cdot V}{m} \quad (2)$$

where C_0 and C_t are the initial and final concentrations of metal ions (mg/L), m is the mass of Mag-Ligand (g), and V is the volume of solution (L).

Mag-Ligand recovery efficiency was calculated as:

$$Recovery\ \ efficiency = \frac{C_w}{C_0} \times 100\% \quad (3)$$

where C_0 (mg/L) is the initial concentrations of Cd^{2+} ions in solution, and C_w (mg/L) is the concentrations of Cd^{2+} ions in the extracted solution (after regeneration).

The Cd^{2+} and Pb^{2+} equilibrium adsorption was evaluated according to Langmuir and Freundlich isotherms using Eq. (4) and Eq. (5), respectively (Morel and Hering, 1993):

$$\frac{C_e}{q_e} = \frac{1}{K_L \cdot q_m} + \frac{C_e}{q_m} \quad (4)$$

$$\log q_e = \log K_F + \frac{1}{n}\log C_e \quad (5)$$

where C_e is solute concentration (mg/L) at equilibrium and q_e is amount adsorbed (mg/g), q_m is the maximum sorption capacity (mg/g). K_L and K_F is the Langmuir and Freundlich sorption equilibrium constant (L/mg), respectively.

Kinetics were analyzed using the pseudo-first-order and pseudo-second-order models using Eq. (6) and Eq. (7) (Coleman et al., 1956):

$$\ln(q_e - q_t) = \ln(q_e) - k_1 t \quad (6)$$

$$\frac{t}{q_t} = \frac{1}{k_2 q_e^2} + \frac{1}{q_e} t \quad (7)$$

where k_1 (h^{-1}) and k_2 ($g/mg\cdot h$) are the equilibrium rate constants of kinetics.

3. Results and discussion

3.1. Mag-Ligand synthesis and characterization

The synthesis of Mag-Ligand consists of two steps, which are schematically presented in Fig. 1. First, the maghemite nanoparticles were coated with APTES to deposit aminopropylalkoxysilane on the surface of the magnetite core. In

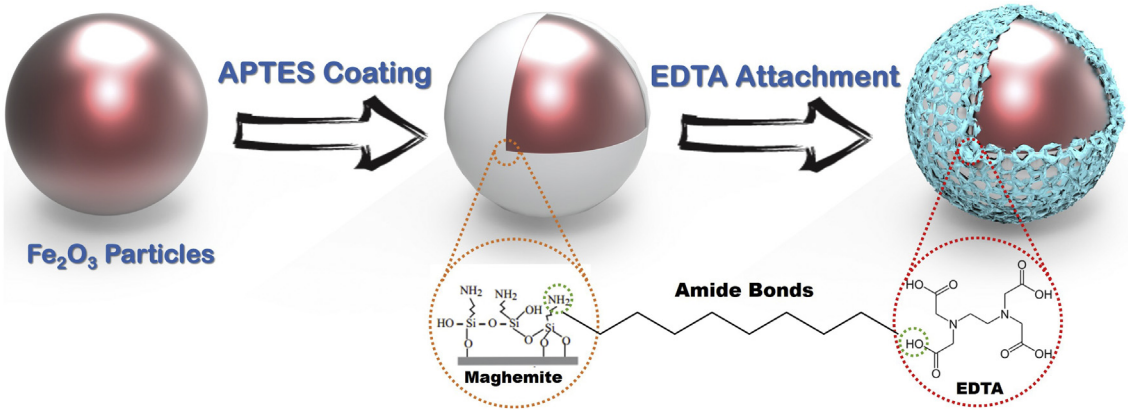

Fig. 1 – Schematic representation of Mag-Ligand synthesis (note: the core and shell are not drawn to scale).

the hydrolysis reaction, the alkoxide groups ($-OC_2H_5$) of APTES were replaced by hydroxyl groups (OH) to form reactive silanol groups, which condensed with other silanol groups to produce siloxane bonds (Si–O–Si) to generate silane polymer (Yamaura et al., 2004). Then these polymers coated the maghemite nanoparticles to form a covalent bond with OH groups (Yamaura et al., 2004). After APTES coating, the maghemite nanoparticles were functionalized with an amino group.

Then, EDTA was attached to the APTES coated maghemite nanoparticles. The covalent attachment of EDTA to particles was achieved by the formation of amide bonds between the carboxylic acid groups of the complexing agent and amino groups provided by the APTES coating (Bernkop-Schnürch and Krajicek, 1998). The SEM micrograph (Fig. 2A and B) shows the porous surface structure of Mag-Ligand. The core/shell structure of Mag-Ligand is shown in the TEM micrograph (Fig. 2C and D), and the shell layer (attached EDTA) is

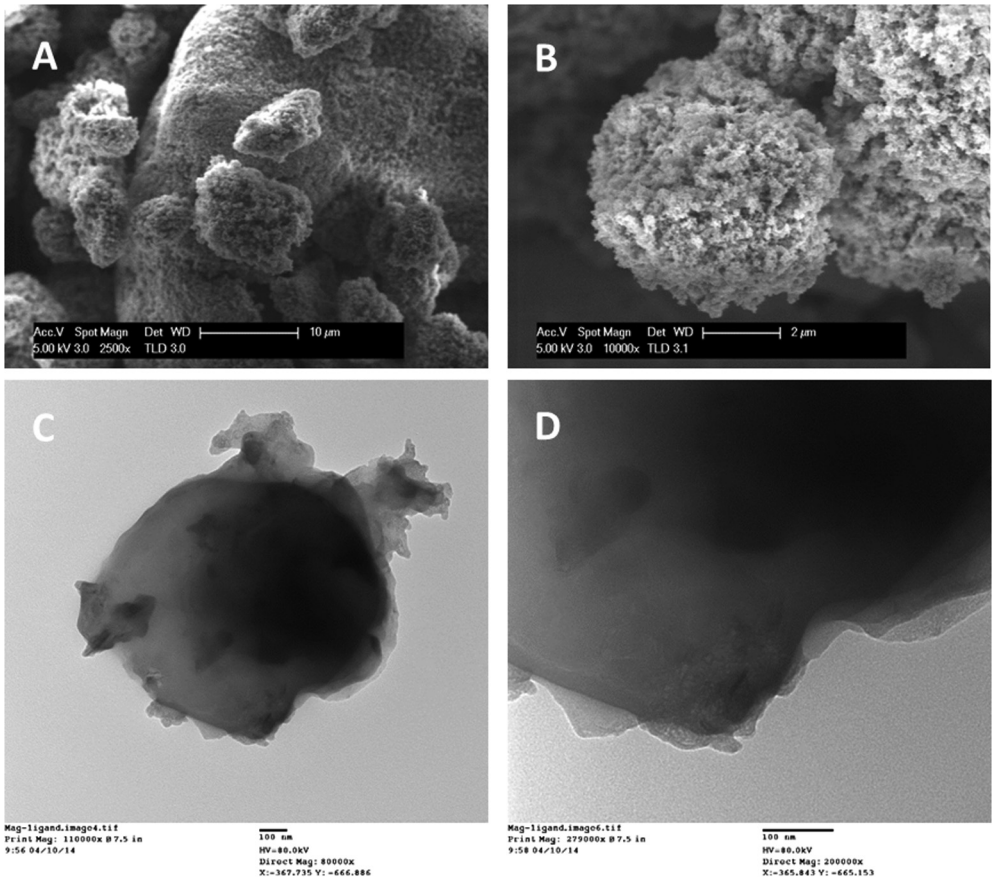

Fig. 2 – (A) SEM micrographs of Mag-Ligand at 2500×, scale bar = 10 μm and (B) at 10,000×, scale bar = 2 μm; (C) TEM micrographs of Mag-Ligand at 80,000×, scale bar = 100 nm and (D) at 200,000, scale bar = 100 nm.

approximately 100 nm as determined by TEM (Fig. 2D). Fig. 2 demonstrates that the hydrated particles are 1–10 μm in size with very high porosity in the nanoscale. Figure S3 (Supplementary Material) indicates that Mag-Ligand is negatively charged (zeta potential from −27 to −47 mV) for pH ranging from 4 to 10.

The FTIR spectra of unmodified maghemite nanoparticles and Mag-Ligand are shown in Fig. 3A. The Mag-Ligand presented peaks for N–H (υ_{N-H}, 3267 cm^{-1}), C=O ($\upsilon_{C=O}$, 1633 cm^{-1}), N–H (υ_{N-H}, 1580 cm^{-1}), C–N (υ_{C-H}, 1400 cm^{-1}) and C–NH_2 (υ_{C-H}, 1119 cm^{-1}); all these functional groups are expected from EDTA. These peaks were not present in the spectra of unmodified maghemite nanoparticles, indicating that the synthesis procedure had successfully attached EDTA on the surface of maghemite nanoparticles.

The TGA curves of as-synthesized Mag-Ligand (Fig. 3B) show four weight loss steps at about 220, 292, 338, 424, and 742 °C, as demonstrated in the derivative curve, which can be ascribed to the decomposition of quaternary ammonium group (Wang et al., 2008), the decomposition of EDTA and transition from Na_2EDTA to Na_2CO_3, the decomposition of Na_2EDTA, and the complete oxidation of carbon, respectively (Wendlandt, 1960). The weight percentage of EDTA attached onto iron oxide particles of Mag-Ligand can be determined by the difference of initial and final mass of the sample in the TGA curve (Fig. 3B) and was approximately 12.5% of the total mass of Mag-Ligand. The high fraction of EDTA and porous surface structure provides many active binding sites for metal ion removal.

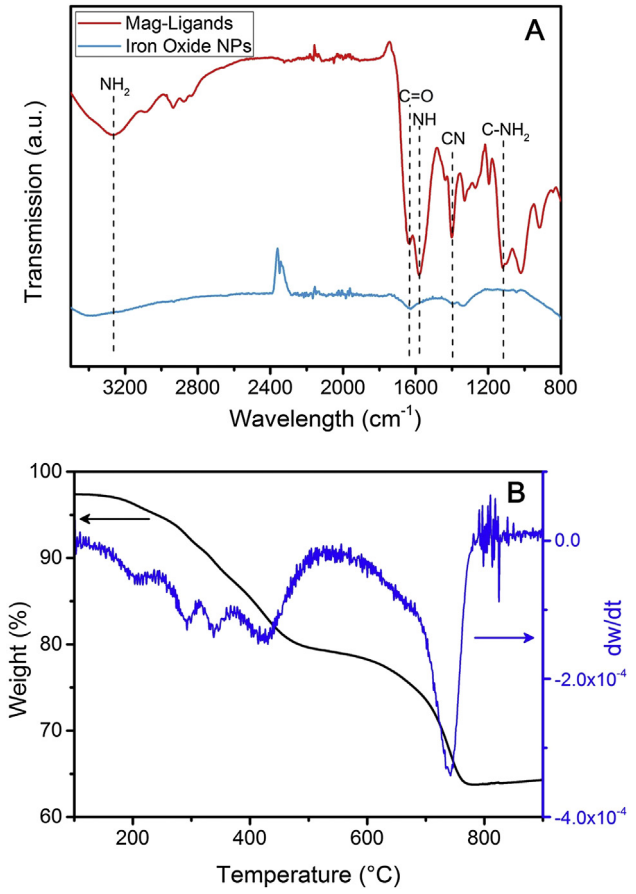

Fig. 3 – (A) FTIR spectra of unmodified magnetite nanoparticles and Mag-Ligand; (B) Thermogravimetric analysis (TGA) of Mag-Ligand.

Magnetic characterization with a superconducting quantum interference device (SQUID) magnetometer at 300 K indicated that maghemite and Mag-Ligand have magnetization saturation values of 59.0 and 52.8 emu/g, respectively (Fig. 4A), indicating a high magnetization. The maghemite content in the macroporous composites is calculated to be as high as 35 weight %. Additionally, no remanence was detected in either maghemite or Mag-Ligand particles, indicating a superparamagnetism feature due to the nanosized maghemite. Due to the strong magnetization, Mag-Ligand suspended in water (0.2 g/L) can be quickly separated from the dispersion with a magnet (1000 Oe), as shown in Fig. 4B and C. These results indicate that the Mag-Ligand possesses excellent magnetic responsivity.

3.2. *Sorption isotherms of Cd and Pb*

Adsorption isotherms of Cd^{2+} and Pb^{2+} onto Mag-Ligand were obtained at pH 7 as shown in Fig. 5. Both Cd^{2+} and Pb^{2+} removal efficiency gradually increased up to the optimum dosage (0.2 and 0.125 g/L for Cd^{2+} and Pb^{2+}, respectively), beyond which the removal efficiency (above 97%) did not change with increasing adsorbent dosage (Fig. 5A), since there are a fixed number of adsorption sites (Sekar et al., 2004).

The effect of initial [Cd^{2+}] (ranging from 1 mg/L to 50 mg/L) and [Pb^{2+}] (ranging from 1 mg/L to 30 mg/L) on adsorption is shown in Fig. 5B. For both ions, removal increased first and then decreased with increasing initial ion concentration, once the maximum adsorption capacity was reached. The initial ion concentration provides the necessary driving force to overcome the resistance to mass transfer of ions between the aqueous

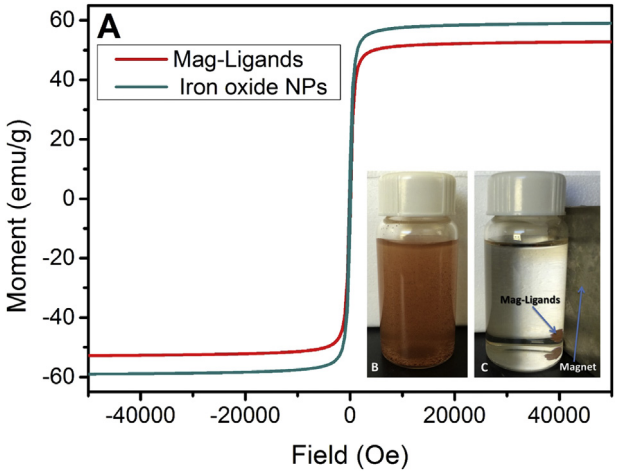

Fig. 4 – (A) The magnetic hysteresis loops of iron oxide nanoparticles and Mag-Ligand; (B) Mag-Ligand particles are introduced into a vial containing contaminated water; (C) A permanent magnet is placed at the side of the vial to attract the magnetic particles, demonstrating the rapid removal of Mag-Ligand from the suspension within seconds of applying a magnetic field.

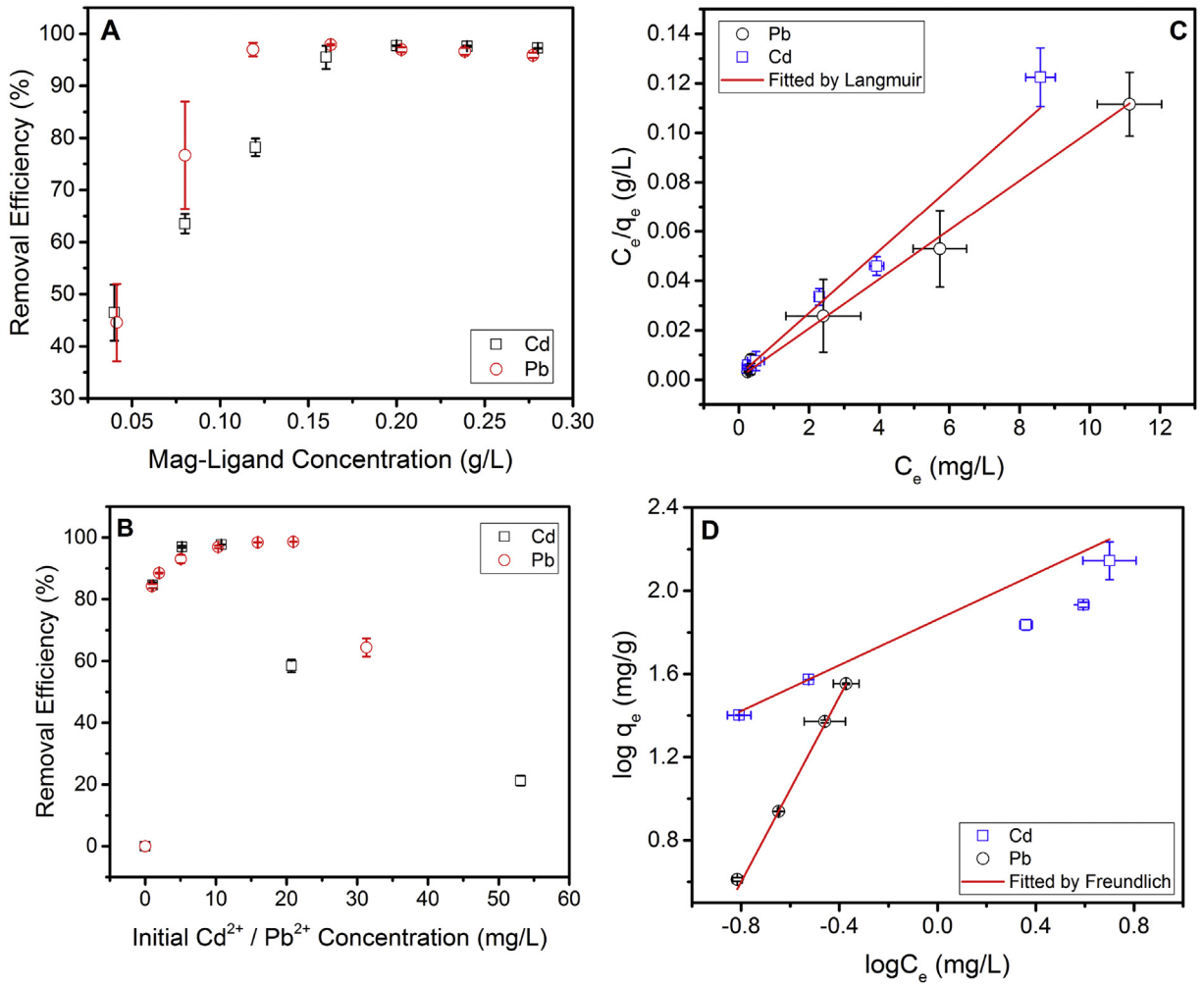

Fig. 5 – Adsorption of Cd^{2+} and Pb^{2+} onto Mag-Ligand (characterized by Cd^{2+} (□) and Pb^{2+} (○)) (A) at pH 7 as a function of adsorbent dose with a fixed initial ions concentration of 10 mg/L; (B) at pH 7 as a function of initial ions concentration with a fixed adsorbent concentration of 2 g/L; (C) Langmuir and (D) Freundlich adsorption isotherms fit at pH 7, symbols represent experimental data, and red line represents model prediction. (For interpretation of the references to color in this figure legend, the reader is referred to the web version of this article.)

and solid phases, and enhances the interaction between Cd^{2+}/Pb^{2+} and Mag-Ligand (Kumar et al., 2010). Fig. 5B indicates that Mag-Ligand has stronger affinity for Pb^{2+} than Cd^{2+}.

The Pb^{2+} and Cd^{2+} isotherm sorption data was fitted using the Langmuir (Fig. 5C) and Freundlich (Fig. 5D) adsorption isotherm models. The Langmuir model provided a slightly better fit for Cd^{2+}, while the Freundlich model fitted Pb^{2+} adsorption better (Table 1). Results of adsorption experiments in this study showed that the maximum adsorption capacity of 79.4 mg/g for Cd^{2+} and 100.2 mg/g for Pb^{2+} onto Mag-Ligand.

Table 1 – Isotherm parameters for Cd^{2+} and Pb^{2+} sorption on Mag-Ligand.

	Langmuir			Freundlich		
	q_m (mg/g)	K_L (L/mg)	R^2	K_F (L/mg)	1/n	R^2
Cd^{2+}	79.365	7.200	0.951	72.755	0.550	0.946
Pb^{2+}	100.200	13.152	0.924	239.939	2.226	0.998

This agrees with the sequence of the EDTA complex formation constants (log K, 25 °C): 18.04 and 16.46 for Pb^{2+} and Cd^{2+}, respectively (Harris, 2010). Table S1 (Supplementary Material) presents a direct comparison between the collected results from this study versus other previously published data of magnetic ligand particles, indicating Mag-Ligand has a higher sorption capacity for Pb^{2+} and Cd^{2+} than previous materials, as well as a wide range of optimum pH.

3.3. *Sorption kinetics of Cd and Pb*

Time dependent removal of metal ions (initial concentration = 10 mg/L) by Mag-Ligand (0.2 g/L) showed rapid adsorption of Cd^{2+} in the first hour (~95% removal efficiency), and thereafter, the adsorption rate decreased gradually. Cd^{2+} equilibrium adsorption was reached (above 97% removal efficiency) in about 2 h (Fig. 6A). Equilibrium for Pb^{2+} was achieved much faster (~15 min) with above 97% removal efficiency, as shown in Fig. 6A. Mag-Ligand has very fast metal

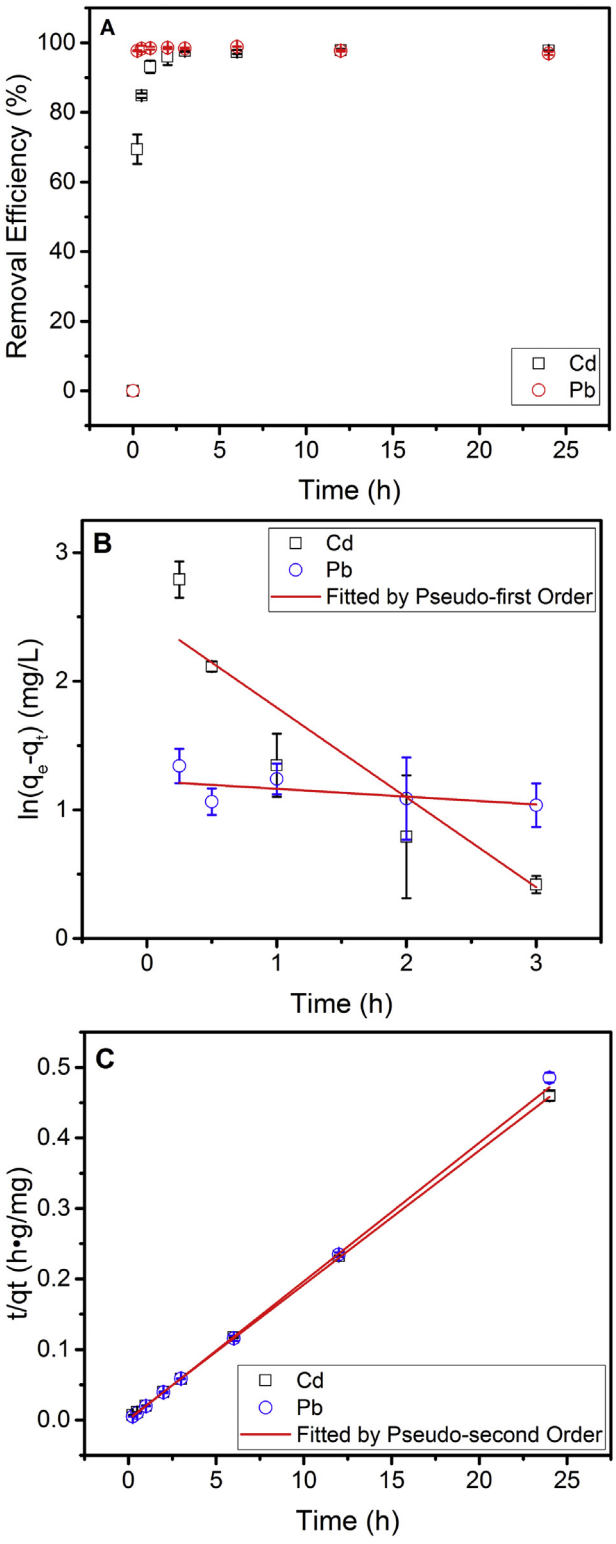

Fig. 6 – Cd^{2+} and Pb^{2+} (A) sorption uptake versus time; and sorption kinetics fitted by (B) Pseudo-first order and (C) Pseudo-second order onto Mag-Ligand in solution at pH 7.

ion sorption kinetics due to the large amount of EDTA accessible to the metal ions in solution, and the difference in kinetics between the metal ions also corresponds with the EDTA affinity sequence (Harris, 2010).

The pseudo-first-order (Fig. 6B) and pseudo-second-order (Fig. 6C) kinetic models were used to investigate the adsorption rate of Cd^{2+} and Pb^{2+} onto Mag-Ligand. The removal of both Cd^{2+} and Pb^{2+} by Mag-Ligand followed pseudo-second order rate ($R^2 > 0.99$) better than pseudo-first-order ($R^2 < 0.88$) (Table 2). The k_2 values (in $g/mg{\cdot}h$) for Cd^{2+} and Pb^{2+} were determined as 0.235 and 7.960, respectively, indicating Mag-Ligand has a much faster removal rate for Pb^{2+} which is due to the stronger binding constant with EDTA (Harris, 2010).

3.4. *Effect of pH on Cd removal*

The influence of pH on the removal efficiency is important in industrial wastewater, particularly for cadmium. No significant difference in Cd^{2+} removal efficiency was found between pH 3 and 7, and the removal efficiency stabilized at around 97% (Fig. 7). Above pH 7, Cd^{2+} removal efficiency decreased gradually as pH increased, to about 86% at pH 10.

Simulation of the aqueous speciation of cadmium using Visual MINTEQ (Gustafsson, 2006) software indicates that for pH from 3 to 10, cadmium in DI water at these concentrations is mostly present as Cd^{2+}. Cd^{2+} has a strong complex formation constant with EDTA (at 25 °C, $Cd^{2+} + EDTA^{4-} \leftrightharpoons Cd\ (EDTA)^{2-}$, $\log K = 14.7$; $Cd\ (EDTA)^{2-} + H^{+} \leftrightharpoons Cd\ (HEDTA)^{-}$, $\log K = 2.5$) (Martell and Smith, 1989), which agrees well with our result: Mag-Ligand showed high removal efficiency across different pH, especially from pH 3 to 7. However, starting from pH 8 there is increasing formation of Cd $(OH)_2$ (Zirino and Yamamoto, 1972), which decreases $Cd(EDTA)^{2-}$ and $Cd(HEDTA)^{-}$ formation.

3.5. *Effect of water hardness on Cd removal*

Water hardness varies in different water matrices, such as tap water, groundwater, river water, lake water and sea water, which is usually expressed as the total amount of Ca^{2+} and Mg^{2+} present in the water. Compared to the trace heavy metal ions, the concentrations of Ca^{2+} and Mg^{2+} ions present in natural water systems is typically much higher, and they can also interact with EDTA to form complexes (Yappert and DuPre, 1997). Fig. 8 shows the removal performance of Cd^{2+} using Mag-Ligand in the presence of different concentrations of Ca^{2+} or Mg^{2+}. No significant difference in Cd^{2+} removal efficiency was found as Mg^{2+} concentration increased up to 60 mg/L in the solution (Fig. 8A). Only at high concentration of Ca^{2+} (above 50 mg/L) was there a decrease in Cd^{2+} removal efficiency (Fig. 8B). These results indicate that Ca^{2+} or Mg^{2+} did not compete strongly with Cd^{2+} in the complexation reaction with EDTA; this agrees with the sequence of the EDTA complex formation constants ($\log K$, 25 °C): 8.79, 10.69 and 16.46 for Mg^{2+}, Ca^{2+} and Cd^{2+}, respectively (Harris, 2010).

Table 2 – Kinetic parameters for Cd^{2+} and Pb^{2+} sorption on Mag-Ligand.

	Pseudo-first order			Pseudo-second order		
	q_e (mg/g)	k_1 (h^{-1})	R^2	q_e (mg/g)	k_2 (g/h·mg)	R^2
Cd^{2+}	12.117	0.699	0.879	52.549	0.235	1.000
Pb^{2+}	3.403	0.061	0.441	50.865	7.960	1.000

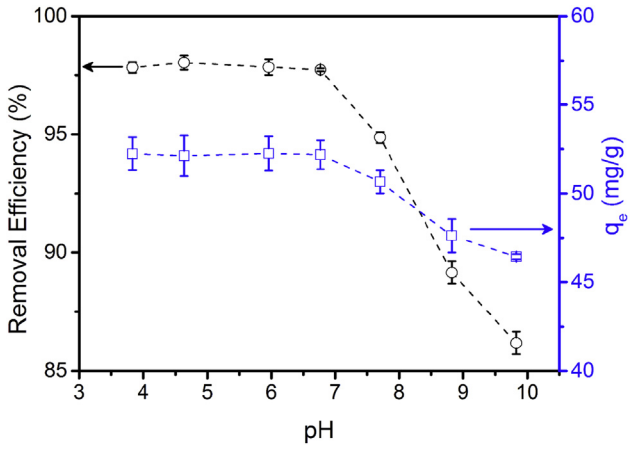

Fig. 7 – Adsorption of Cd^{2+} onto Mag-Ligand in solution as a function of pH, characterized by the removal efficiency (○) and adsorption capacity (□).

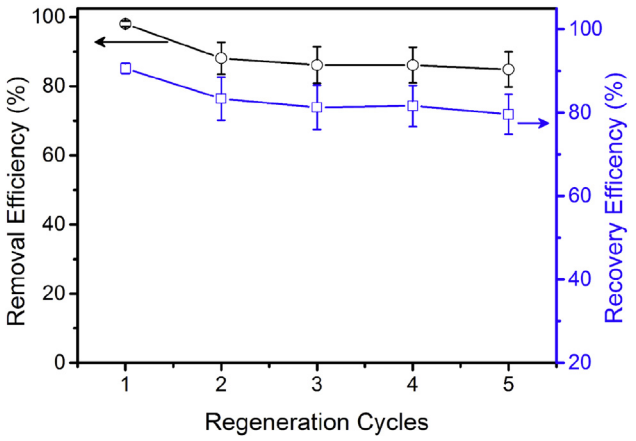

Fig. 9 – Cd^{2+} (10 mg/L initial concentration) removal efficiency (○) from solution and Cd^{2+} recovery (□) from Mag-Ligand during five regeneration cycles.

3.6. *Regeneration and reuse of Mag-Ligand*

To demonstrate the regenerability and reusability of the Mag-Ligand, the recovery of Cd^{2+} sorbed onto the Mag-Ligand was investigated using a 1% HCl wash. Cd^{2+} removal and Mag-Ligand recovery during five continuous cycles of regeneration and reuse are shown in Fig. 9. It was found that a large fraction of the sorbed Cd^{2+} (>80%, over 8 mg/L) could be recovered, indicating easy regeneration of Mag-Ligand (Fig. 9). Some loss (within 10% change) of Cd^{2+} sorption capacity was observed for the regenerated Mag-Ligand after 5 cycles (Fig. 9), indicating good reusability of Mag-Ligand. The decreased chelating capacity was likely due to irreversibly bound metals or loss of chelator (Koehler et al., 2009).

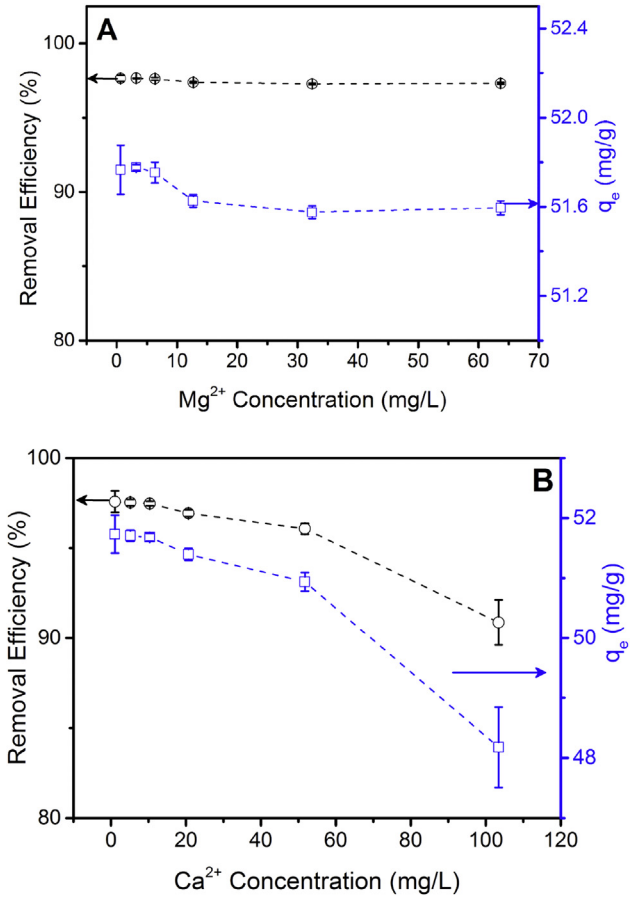

Fig. 8 – Adsorption of Cd^{2+} (10 mg/L initial concentration) onto Mag-Ligand (removal efficiency (○) and adsorption capacity (□)) in the presence of (A) Mg^{2+} (from 0.6 mg/L to 60 mg/L) and (B) Ca^{2+} (from 1 mg/L to 100 mg/L) at pH 7.

4. Conclusions

Mag-Ligand represents a significant improvement in metal ion decontamination in a wide range of aqueous matrices, since (1) Mag-Ligand only requires a simple synthesis procedure and exhibits high metal ion removal capacity; (2) the superparamagnetic Fe_2O_3 core allows rapid separation of Mag-Ligand after sorption; (3) Mag-Ligand can be easily recovered, regenerated and reused, significantly increasing treatment efficiency and reducing operation cost; (4) Mag-Ligand exhibits high removal efficiency under different environmental conditions (e.g. pH range from 4 to 10; up to 60 mg/L Ca^{2+} or Mg^{2+} present in the solution); (5) the residual Cd^{2+} and Pb^{2+} in solution represents a very small fraction of the initial contaminated mass and volume; and (6) sorption kinetics indicate fast removal of metal ions. The most likely mechanisms of Cd^{2+}adsorption onto Mag-Ligand are (1) complexation reactions with EDTA and (2) adsorption of Cd^{2+} or Pb^{2+} on the surface porous structures. Future work will address the current synthesis process, seeking a more sustainable approach with an aqueous-based synthesis.

Therefore, Mag-Ligand are reusable sorbents for the fast, convenient, and highly efficient removal of Cd^{2+} and Pb^{2+} from contaminated aquatic systems. It is expected that the Mag-Ligand will have potentially wide application in the removal of other heavy metal pollutants from aquatic systems.

Acknowledgments

This work made use of MRL Central Facilities supported by the MRSEC Program of the National Science Foundation under awards NO. DMR 1121053; a member of the NSF-funded Materials Research Facilities Network (www.mrfn.org). We thank the MRL Central Facilities for the use of their ICP, TGA, SEM, FTIR and SQUID instruments and Amanda Strom at the UCSB MRL for her help with these instruments. We also thank Hiroaki Kiyoto for initial work in this project, and the anonymous reviewers for their valuable comments, and acknowledge the lab assistance of Aaron Fulton.

Appendix A. Supplementary data

Supplementary data related to this article can be found at http://dx.doi.org/10.1016/j.watres.2015.05.011.

REFERENCES

Adeleye, A., Keller, A., Miller, R., Lenihan, H., 2013. Persistence of commercial nanoscaled zero-valent iron (nZVI) and by-products. J. Nanoparticle Res. 15 (1), 1–18.

Adeleye, A.S., Keller, A.A., 2014. Long-term colloidal stability and metal leaching of single wall carbon nanotubes: effect of temperature and extracellular polymeric substances. Water Res. 49 (0), 236–250.

Alvarez, S.M., Gomez, N.N., Scardapane, L., Zirulnik, F., Martinez, D., Gimenez, M.S., 2004. Morphological changes and oxidative stress in rat prostate exposed to a non-carcinogenic dose of cadmium. Toxicol. Lett. 153 (3), 365–376.

Bagheri, H., Afkhami, A., Saber-Tehrani, M., Khoshsafar, H., 2012. Preparation and characterization of magnetic nanocomposite of Schiff base/silica/magnetite as a preconcentration phase for the trace determination of heavy metal ions in water, food and biological samples using atomic absorption spectrometry. Talanta 97, 87–95.

Bandara, J.M.R.S., Senevirathna, D.M.A.N., Dasanayake, D.M.R.S.B., Herath, V., Bandara, J.M.R.P., Abeysekara, T., Rajapaksha, K.H., 2008. Chronic renal failure among farm families in cascade irrigation systems in Sri Lanka associated with elevated dietary cadmium levels in rice and freshwater fish (Tilapia). Environ. Geochem. Health 30 (5), 465–478.

Bernkop-Schnürch, A., Krajicek, M.E., 1998. Mucoadhesive polymers as platforms for peroral peptide delivery and absorption: synthesis and evaluation of different chitosan–EDTA conjugates. J. Control. Release 50 (1), 215–223.

Bonda, E., Wlostowski, T., Krasowska, A., 2004. Testicular toxicity induced by dietary cadmium is associated with decreased testicular zinc and increased hepatic and renal metallothionein and zinc in the bank vole (*Clethrionomys glareolus*). Biometals 17 (6), 615–624.

Boudreau, J., Vincent, R., Nadeau, D., Trottier, B., Fournier, M., Krzystyniak, K., Chevalier, G., 1988. Toxicity of inhaled cadmium chloride – early responses of the antioxidant and surfactant systems in rat lungs. J. Toxicol. Environ. Health 23 (2), 241–256.

Clark, K.K., Keller, A.A., 2012a. Adsorption of perchlorate and other oxyanions onto magnetic permanently confined micelle arrays (Mag-PCMAs). Water Res. 46 (3), 635–644.

Clark, K.K., Keller, A.A., 2012b. Investigation of two magnetic permanently confined micelle array sorbents using nonionic and cationic surfactants for the removal of PAHs and pesticides from aqueous media. Water, Air, & Soil Pollut. 223 (7), 3647–3655.

Coleman, N.T., Mcclung, A.C., Moore, D.P., 1956. Formation constants for Cu(Ii)-peat complexes. Science 123 (3191), 330–331.

Faraji, M., Yamini, Y., Saleh, A., Rezaee, M., Ghambarian, M., Hassani, R., 2010. A nanoparticle-based solid-phase extraction procedure followed by flow injection inductively coupled plasma-optical emission spectrometry to determine some heavy metal ions in water samples. Anal. Chim. Acta 659 (1–2), 172–177.

Fthenakis, V.M., 2004. Life cycle impact analysis of cadmium in CdTe PV production. Renew. Sustain. Energy Rev. 8 (4), 303–334.

Ge, F., Li, M.M., Ye, H., Zhao, B.X., 2012. Effective removal of heavy metal ions Cd2+, Zn2+, Pb2+, Cu2+ from aqueous solution by polymer-modified magnetic nanoparticles. J. Hazard. Mater. 211, 366–372.

Gustafsson, J.P., 2006. Visual minteq. Capturado em de 26.

Harris, D.C., 2010. Quantitative Chemical Analysis. Macmillan.

Huang, Y.F., Li, Y., Jiang, Y., Yan, X.P., 2010. Magnetic immobilization of amine-functionalized magnetite microspheres in a knotted reactor for on-line solid-phase extraction coupled with ICP-MS for speciation analysis of trace chromium. J. Anal. Atom. Spectrom. 25 (9), 1467–1474.

Huang, Y.X., Keller, A.A., 2013. Magnetic nanoparticle adsorbents for emerging organic contaminants. ACS Sustain. Chem. Eng. 1 (7), 731–736.

Huang, Y.X., Yang, J.K., Keller, A.A., 2014. Removal of arsenic and phosphate from aqueous solution by metal (hydr-)oxide coated sand. ACS Sustain. Chem. Eng. 2 (5), 1128–1138.

Hughes, M.A., Rosenherg, E., 2007. Characterization and applications of poly-acetate modified silica polyamine composites. Sep. Sci. Technol. 42 (2), 261–283.

Islamoglu, S., Yilmaz, L., Ozbelge, H.O., 2006. Development of a precipitation based separation scheme for selective removal and recovery of heavy metals from cadmium rich electroplating industry effluents. Sep. Sci. Technol. 41 (15), 3367–3385.

Júnior, O.K., Gurgel, L.V.A., de Freitas, R.P., Gil, L.F., 2009. Adsorption of Cu (II), Cd (II), and Pb (II) from aqueous single metal solutions by mercerized cellulose and mercerized sugarcane bagasse chemically modified with EDTA dianhydride (EDTAD). Carbohydr. Polym. 77 (3), 643–650.

Jamall, I.S., Naik, M., Sprowls, J.J., Trombetta, L.D., 1989. A comparison of the effects of dietary-cadmium on heart and kidney antioxidant enzymes – evidence for the greater vulnerability of the heart to cadmium toxicity. J. Appl. Toxicol. 9 (5), 339–345.

Jiang, H.M., Yan, Z.P., Zhao, Y., Hu, X., Lian, H.Z., 2012. Zincon-immobilized silica-coated magnetic Fe3O4 nanoparticles for solid-phase extraction and determination of trace lead in natural and drinking waters by graphite furnace atomic absorption spectrometry. Talanta 94, 251–256.

Kah, M., Levy, L., Brown, C., 2012. Potential for effects of land contamination on human health. 1. The case of cadmium. J. Toxicol. Environ. Health Part B Crit. Rev. 15 (5), 348–363.

Karatapanis, A.E., Fiamegos, Y., Stalikas, C.D., 2011. Silica-modified magnetic nanoparticles functionalized with cetylpyridinium bromide for the preconcentration of metals after complexation with 8-hydroxyquinoline. Talanta 84 (3), 834–839.

Koehler, F.M., Rossier, M., Waelle, M., Athanassiou, E.K., Limbach, L.K., Grass, R.N., Gunther, D., Stark, W.J., 2009. Magnetic EDTA: coupling heavy metal chelators to metal

nanomagnets for rapid removal of cadmium, lead and copper from contaminated water. Chem. Commun. 32, 4862–4864.
Koyuturk, M., Yanardag, R., Bolkent, S., Tunali, S., 2007. The potential role of combined anti-oxidants against cadmium toxicity on liver of rats. Toxicol. Indust. Health 23 (7), 393–401.
Kumar, P.S., Ramalingam, S., Senthamarai, C., Niranjanaa, M., Vijayalakshmi, P., Sivanesan, S., 2010. Adsorption of dye from aqueous solution by cashew nut shell: studies on equilibrium isotherm, kinetics and thermodynamics of interactions. Desalination 261 (1–2), 52–60.
Martell, A.E., Smith, R.M., 1989. Critical Stability Constants. Springer.
Martinez, M., Miralles, N., Hidalgo, S., Fiol, N., Villaescusa, I., Poch, J., 2006. Removal of lead(II) and cadmium(II) from aqueous solutions using grape stalk waste. J. Hazard. Mater. 133 (1–3), 203–211.
Morel, F.M.M., Hering, J.G., 1993. Principles and Applications of Aquatic Chemistry. Wiley.
Mortvedt, J.J., Osborn, G., 1982. Studies on the chemical form of cadmium contaminants in phosphate fertilizers. Soil Sci. 134 (3), 185–192.
Ngah, W.S.W., Hanafiah, M.A.K.M., 2008. Removal of heavy metal ions from wastewater by chemically modified plant wastes as adsorbents: a review. Bioresour. Technol. 99 (10), 3935–3948.
Pereira, F.V., Gurgel, L.V.A., Gil, L.F., 2010. Removal of Zn^{2+} from aqueous single metal solutions and electroplating wastewater with wood sawdust and sugarcane bagasse modified with EDTA dianhydride (EDTAD). J. Hazard. Mater. 176 (1–3), 856–863.
Reimann, C., de Caritat, P., 2005. Distinguishing between natural and anthropogenic sources for elements in the environment: regional geochemical surveys versus enrichment factors. Sci. Total Environ. 337 (1–3), 91–107.
Repo, E., Kurniawan, T.A., Warchol, J.K., Sillanpaa, M.E.T., 2009. Removal of Co(II) and Ni(II) ions from contaminated water using silica gel functionalized with EDTA and/or DTPA as chelating agents. J. Hazard. Mater. 171 (1–3), 1071–1080.
Repo, E., Warchol, J.K., Bhatnagar, A., Sillanpaa, M., 2011. Heavy metals adsorption by novel EDTA-modified chitosan-silica hybrid materials. J. Colloid Interface Sci. 358 (1), 261–267.
Repo, E., Warchol, J.K., Kurniawan, T.A., Sillanpaa, M.E.T., 2010. Adsorption of Co(II) and Ni(II) by EDTA- and/or DTPA-modified chitosan: kinetic and equilibrium modeling. Chem. Eng. J. 161 (1–2), 73–82.
Sekar, M., Sakthi, V., Rengaraj, S., 2004. Kinetics and equilibrium adsorption study of lead(II) onto activated carbon prepared from coconut shell. J. Colloid Interface Sci. 279 (2), 307–313.
Shute, T., Macfie, S.M., 2006. Cadmium and zinc accumulation in soybean: a threat to food safety? Sci. Total Environ. 371 (1–3), 63–73.
Su, Y., Adeleye, A.S., Keller, A.A., Huang, Y., Dai, C., Zhou, X., Zhang, Y., 2015. Magnetic sulfide-modified nanoscale zerovalent iron (S-nZVI) for dissolved metal ion removal. Water Res. 74, 47–57.
Su, Y.M., Adeleye, A.S., Huang, Y.X., Sun, X.Y., Dai, C.M., Zhou, X.F., Zhang, Y.L., Keller, A.A., 2014. Simultaneous removal of cadmium and nitrate in aqueous media by nanoscale zerovalent iron (nZVI) and Au doped nZVI particles. Water Res. 63, 102–111.
Tête, N., Durfort, M., Rieffel, D., Scheifler, R., Sánchez-Chardi, A., 2014. Histopathology related to cadmium and lead bioaccumulation in chronically exposed wood mice, Apodemus sylvaticus, around a former smelter. Sci. Total Environ. 481, 167–177.
Vouk, V.B., Piver, W.T., 1983. Metallic elements in fossil-fuel combustion products – amounts and form of emissions and evaluation of carcinogenicity and mutagenicity. Environ. Health Perspect. 47 (Jan), 201–225.
Vromman, V., Saegerman, C., Pussemier, L., Huyghebaert, A., Temmerman, L.D., Pizzolon, J.-C., Waegeneers, N., 2008. Cadmium in the food chain near non-ferrous metal production sites. Food Addit. Contam. 25 (3), 293–301.
Wang, H., Keller, A.A., Clark, K.K., 2011. Natural organic matter removal by adsorption onto magnetic permanently confined micelle arrays. J. Hazard. Mater. 194, 156–161.
Wang, L.Y., Yang, L.Q., Li, Y.F., Zhang, Y., Ma, X.J., Ye, Z.F., 2010. Study on adsorption mechanism of Pb(II) and Cu(II) in aqueous solution using PS-EDTA resin. Chem. Eng. J. 163 (3), 364–372.
Wang, P., Shi, Q., Shi, Y., Clark, K.K., Stucky, G.D., Keller, A.A., 2008. Magnetic permanently confined micelle arrays for treating hydrophobic organic compound contamination. J. Am. Chem. Soc. 131 (1), 182–188.
Wendlandt, W.W., 1960. Thermogravimetric and differential thermal analysis of (ethylenedinitrilo)tetraacetic acid and its derivatives. Anal. Chem. 32 (7), 848–850.
Xie, Y., Giammar, D.E., 2011. Effects of flow and water chemistry on lead release rates from pipe scales. Water Res. 45 (19), 6525–6534.
Xiong, Z.G., Zhang, L.L., Ma, J.Z., Zhao, X.S., 2010. Photocatalytic degradation of dyes over graphene-gold nanocomposites under visible light irradiation. Chem. Commun. 46 (33), 6099–6101.
Yamaura, M., Camilo, R.L., Sampaio, L.C., Macedo, M.A., Nakamura, M., Toma, H.E., 2004. Preparation and characterization of (3-aminopropyl) triethoxysilane-coated magnetite nanoparticles. J. Magnet. Mag. Mater. 279 (2–3), 210–217.
Yappert, M.C., DuPre, D.B., 1997. Complexometric titrations: competition of complexing agents in the determination of water hardness with EDTA. J. Chem. Educ. 74 (12), 1422–1423.
Yu, J.X., Tong, M., Sun, X.M., Li, B.H., 2008. Enhanced and selective adsorption of Pb2+ and Cu2+ by EDTAD-modified biomass of baker's yeast. Bioresour. Technol. 99 (7), 2588–2593.
Zirino, A., Yamamoto, S., 1972. A pH-dependent model for the chemical speciation of copper, zinc, cadmium and lead in seawater. Limnol. Oceanogr. 17 (5), 661–671.